PROCEEDINGS OF THE 14TH SYMPOSIUM ON THE GEOLOGY OF THE BAHAMAS AND OTHER CARBONATE REGIONS

Edited by
Fredrick D. Siewers and Jonathan B. Martin

Production Editor:
Fredrick D. Siewers

Front Cover Photograph – "Kelly and the Veggiemorphs" courtesy of Jon Martin

Back Cover Photograph – "Luigi" courtesy of Erin Rothfus

FURTHER EVIDENCE FOR A +20 M SEA-LEVEL HIGHSTAND DURING MARINE ISOTOPE STAGE 11 FROM FOSSIL LACUSTRINE SEDIMENTS: GLASS WINDOW, ELEUTHERA, BAHAMAS

Fabienne Godefroid
Section of Earth and Environmental Sciences
University of Geneva
1205 Geneva, Switzerland
fabienne.godefroid@unige.ch

Pascal Kindler and Carole Nawratil de Bono
Section of Earth and Environmental Sciences
University of Geneva
1205 Geneva, Switzerland

ABSTRACT

Fossil lacustrine sediments were found at about 15 m above sea level, directly above beach deposits dating from Marine Isotope Stage (MIS) 11 on a tectonically stable coastline in Eleuthera (Bahamas). This new discovery brings further support to the hypothesis suggesting that a major collapse of polar ice sheets occurred during this interglacial period.

Two stratigraphic sections (GW1/GW2), including several carbonate units separated by paleosols, were logged near Glass Window (northern Eleuthera). Both sections comprise a basal unit of cross-bedded, bio-peloidal limestone, containing an early generation of fibrous rim cement of marine origin and a late phase of drusy calcite mosaic cement. A second overlying unit displays well-defined planar bedding at both sites, whereas faint trough cross-stratifications are also visible at GW1. This second unit consists of a bio-peloidal grainstone containing *Halimeda* fragments and lithoclasts derived from the underlying unit, and is further characterized by an early generation of isopachous fibrous cement. The upper part of this second unit is dismantled in dm-sized blocks which are encrusted by a thick micritic crust con-taining algal remains and spherulites of cyanobacterial origin. The top of the GW2 section is represented by a karstified oolitic/peloidal grainstone, not found at GW 1, whereas the upper part of GW1 includes one bioclastic and one oolitic limestone unit separated by a paleosol.

Based on sedimentary structures, petrographic composition, and amino-acid ratios borrowed from previous authors, the lower and upper units exposed at both sections can be identified as eolianites dating from MIS 11, 9, 7 and 5e, respectively. Occurring between 12 and 14.5 meters above sea level (masl), the basal part of the second unit can be interpreted as a beach deposit, whereas its upper part, at 15 masl, likely corresponds to lacustrine or pond sediments, both dating from MIS 11. Considering the subsidence rate affecting Eleuthera, these beach and pond deposits, and the phreatic cements in the basal eolian units imply a sea-level highstand at ca. 20 masl during MIS 11. This exceptional event was probably caused by the collapse and melting of polar ice-sheets during this very warm climatic period. In the context of present-day global warming, a similar scenario could be repeated in the near future.

INTRODUCTION

The Bahamas archipelago is a unique and ideal region for carbonate sedimentology and the study of Quaternary eustatic and climatic changes. On several islands, subvertical carbonate cliffs preserve a pristine sedimentary record enabling the reconstruction of ancient depositional environments and paleoenvironmental change since the middle Pleistocene. Recently, Hearty et al. (1999) and Kindler and Hearty (2000) described vertically stacked beach and eolian deposits in northern Eleuthera, and correlated them with sea-level highstands at 2, 7 and 20 m above sea level (masl) during Marine Isotope Stage (MIS) 11. According to several authors (Howard, 1997; Droxler et al., 1999; Poore et al., 1999), this time period corresponds to the longest (420 to 360 ka) and warmest interglacial of the past 500 kyr, and is indeed characterized by exceptional elevations of the sea, due to the pronounced melting of polar ice sheets. In addition to the Bahamian cases, elevated marine deposits dating from MIS 11 have been reported by Bowen (1999; 23 masl in southern Britain), Brigham-Grette (1999; 22-23 masl in NW Alaska), Hearty et al. (1999; 22 masl in Bermuda), Olson and Hearty (2009; 21 masl in Bermuda), and Hearty (2002, 2007; 20 masl in Hawaii). These discoveries and interpretations have been strongly challenged. Indeed, McMurtry et al. (2008) and Mylroie (2008) claim that these elevated marine deposits result from high-energy oceanographic events (tsunamis, storm surges), and are inconsistent with intertidal deposition, which would suggest an important deglaciation. Moreover, Hodell et al. (2000) and Kandiano and Bauch (2007) contend that such a high sea level is not supported by benthic and planktonic oxygen-isotope values from deep-sea sediments.

In this paper, we describe and interpret two stratigraphic sections from the Glass Window area in Eleuthera which include beach deposits exposed between 12 and 14.5 masl, capped by low-energy lacustrine sediments at +15 masl, both

correlated with MIS 11. These new data bring further support to the aforementioned reports of exceptional sea levels during this interglacial, which appears as the best candidate for providing a credible scenario for some outcomes of human-induced global warming.

SETTING AND METHODS

Eleuthera is an elongated and narrow (140 x 2-5 km) carbonate island located along the NE edge of Great Bahama Bank (GBB; Fig. 1). Spectacular high cliffs and peculiar geological features, especially in the northern part of the island, have triggered the interest of many geologists in the past three decades (e.g. Ball, 1967; Kindler and Hearty, 1995; 1997; Hearty 1997, 1998; Hearty and Kaufmann, 2000; Mylroie, 2008). The northeastern part of GBB is considered as tectonically passive (Sheridan et al., 1988) and is only affected by slow (1.6 cm/10^3 years; Lynts, 1970; Mullins and Lynts, 1977; Carew and Mylroie, 1995) subsidence linked to thermally induced sedimentary loading (Pindell, 1985). Possibly active compressive features, related to the slow convergence between North and South America, have nonetheless been observed in the subsurface to the West
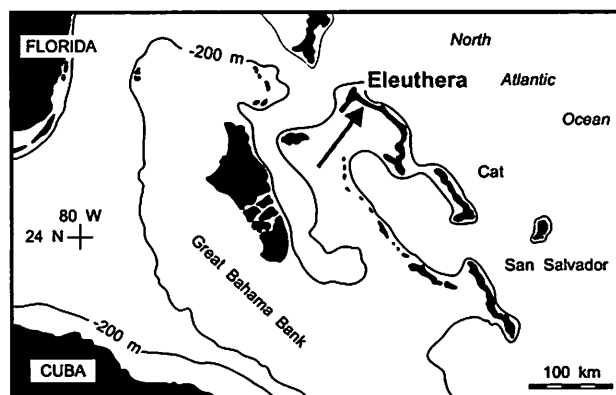

Figure 1: Sketch map of the northwestern Bahamas showing the location of Eleuthera. The studied area, Glass Window, is located near the northern end of this island (arrow).

of GBB (Masaferro et al., 1999). The stratigraphic record from the Bahamas archipelago includes two types of lithological units: (1) terra-rossa paleosols which form mostly during glacial periods, when the banks are exposed (Carew and Mylroie, 1997), and (2) carbonate units, of diverse lithologic composition (Kindler and Hearty, 1996), which characterize interglacial times, when the platforms are submerged. The majority of carbonate units is represented by eolianites and high-energy marine deposits including subtidal and beach facies. By contrast, low-energy sediments (e.g. lagoonal, tidal flat, lacustrine) have rarely been described in the fossil record exposed on the islands (Hagey and Mylroie, 1995; Noble et al., 1995).

Numerous vertically stacked lithological units crop out in the Glass Window area. These have been studied by several authors (Kindler and Hearty, 1997; Hearty, 1998; Michaud, 1999; Panuska et al., 2002; Nawratil de Bono 2008), but observations and interpretations are conflicting. Therefore, we performed a detailed stratigraphic and sedimentological logging of two sections (GW1/GW2; Fig. 2) to complement and clarify previous data. Located at about 100 m to the north of the Glass Window bridge, the GW1 section (coord. 25°26'17.64"N and 76°36'17.39"W; Fig. 3) is a 22 m-high sea cliff that must not be explored during rough weather. GW2 (coord. 25°26'12.99"N and 76°36'09.28"W; Fig. 4) corresponds to a lagoon-facing road cut situated at about 100 m to the south of the GW bridge. Sampling was made at closely spaced intervals. All samples were thin sectioned and examined with a polarizing microscope to identify constituent grains and cements, which is important for determining the depositional setting and the early diagenetic history of the rocks. In addition, small box cores were collected in modern low-energy environments on San Salvador to compare these sediments with potential fossil counterparts. Our geochronological interpretation relies on amino-acid racemization (AAR) data obtained from whole-rock samples by Hearty (1998) and Nawratil de
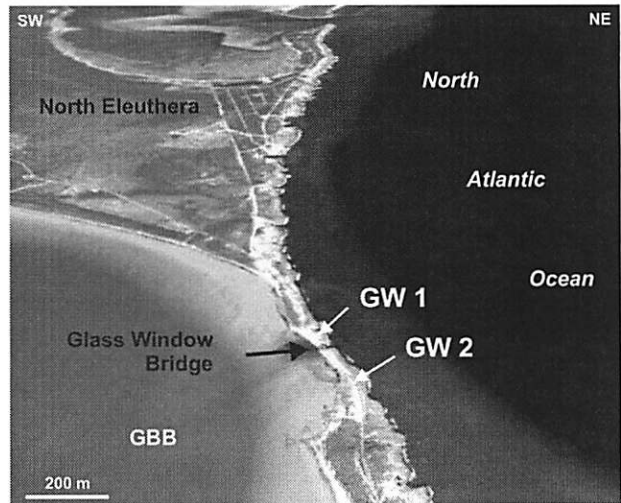

Figure 2:Oblique air view showing the locations of the two studied sections (GW1 and GW2) in the Glass Window area which is situated on Fig. 1 (GBB = Great Bahama Bank; source Google Earth).

Bono (2008). The AAR method is based on the interconversion of amino acids from one chiral form (the L -laevo amino acids-) to a mixture of L- and D- (dextro) forms. The extent of racemization is measured by the ratio of D/L isomers and increases as a function of time and temperature. In our case, we used the ratio of D-alloisoleucine/L-isoleucine (or A/I ratio) to get a relative age of carbonate units and refine stratigraphic correlations. Details on the whole-rock AAR method can be found in Hearty et al. (1992) and Hearty and Kaufmann (2000).

RESULTS

Physical stratigraphy

Section GW1 (Figs. 3 and 5) exposes four distinctive carbonate units separated by reddish paleosols, studied in detail by Nawratil de Bono (2008), and/or erosional surfaces.

Unit 1 is visible from sea level up to an elevation of 12 to 14 m. It is subdivided into two
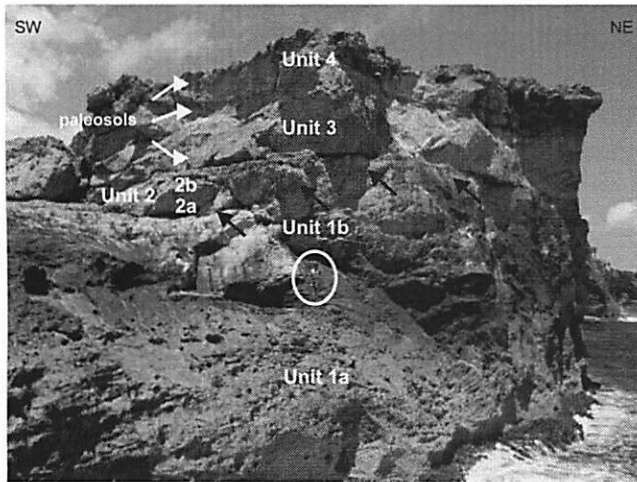
Figure 3: View of the GW1 section showing verti-cally stacked carbonate units and paleosols (white arrows). Black arrows point to the erosional sur-face between Units 1 and 2. Note large, steeply dipping foresets in Unit 1b. Cliff is 22 m high. Person for scale (circled) is 1.58 m tall.

Figure 4: General view of the GW2 section. Note erosional surface truncating Unit A (white ar-rows), and convex-up cross-bedding in this unit. Dotted line emphasizes the boundary between Unit B2 and C; hammer length = 36 cm.

units (1a and 1b) by a subhorizontal surface that is best seen at about 6 masl on the SE side of the exposure. Unit 1a is made of a well-lithified, lam-inated, bioclastic-peloidal grainstone exhibiting moderately inclined foresets dipping in a bank-ward direction (Fig. 3) and rare fenestral poros-ity. Most represented bioclasts include *Halimeda* fragments and porcellaneous foraminifers (e.g. Peneroplids). Cement (up to 30% of the rock vol-ume) comprises partly preserved, early fibrous or bladed fringes rimming the grains (Fig. 6), and late low-Mg calcite crystals filling pores and de-veloping polygonal boundaries. Samples collect-ed just below the aforementioned surface at +6 m further display petrographic features of pedogenic origin (soil pisoids and micritized zones; Bain and Foos, 1993). Unit 1b comprises a well-lithified, peloidal-bioclastic grainstone showing meter-scale foresets dipping towards the S-SW with a ca. 40° angle (Fig. 3). The petrographic composition and cementation pattern of this unit is very similar to that of Unit 1a, except for the predominance of peloids over bioclasts (Fig. 7).
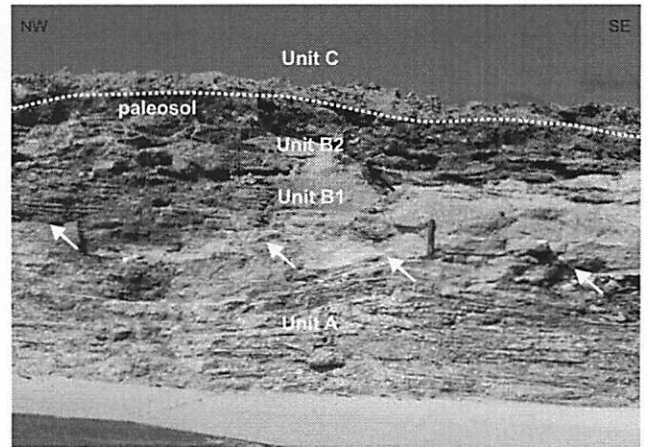
Unit 2 is exposed between 12 and 15 m. It

is separated from Unit 1 by an erosional surface, which truncates the underlying foresets, and is capped by a 50 cm-thick, sandy paleosol studied by Nawratil de Bono (2008). This unit can also be subdivided in two parts. Unit 2a is made of a coarse-grained, laminated, bioclastic grainstone showing low-angle, trough-cross bedding at the base of the unit (Fig. 8) and, higher up, large-scale planar cross-beds dipping towards the SW with a low angle, and containing rare fenestrae. Predominant constituents include *Halimeda* frag-ments, porcellaneous benthic foraminifers, and rounded lithoclasts made of peloidal grainstone, likely derived from Unit 1 (Fig. 9). The cement pattern of this rock contains an early generation of fibrous isopachous rims (partly preserved and recrystallized), overlain by thin, non-isopachous rims of undulating micrite, and a late generation of sparry calcite filling pores and/or forming me-nisci at grain contacts (Figs. 9 and 10). Unit 2b represents the upper 20 to 50 cm of Unit 2, where the bioclastic grainstone composing this unit is capped and penetrated by a cm-thick laminated crust. This crust exhibits two kinds of mm-scale,
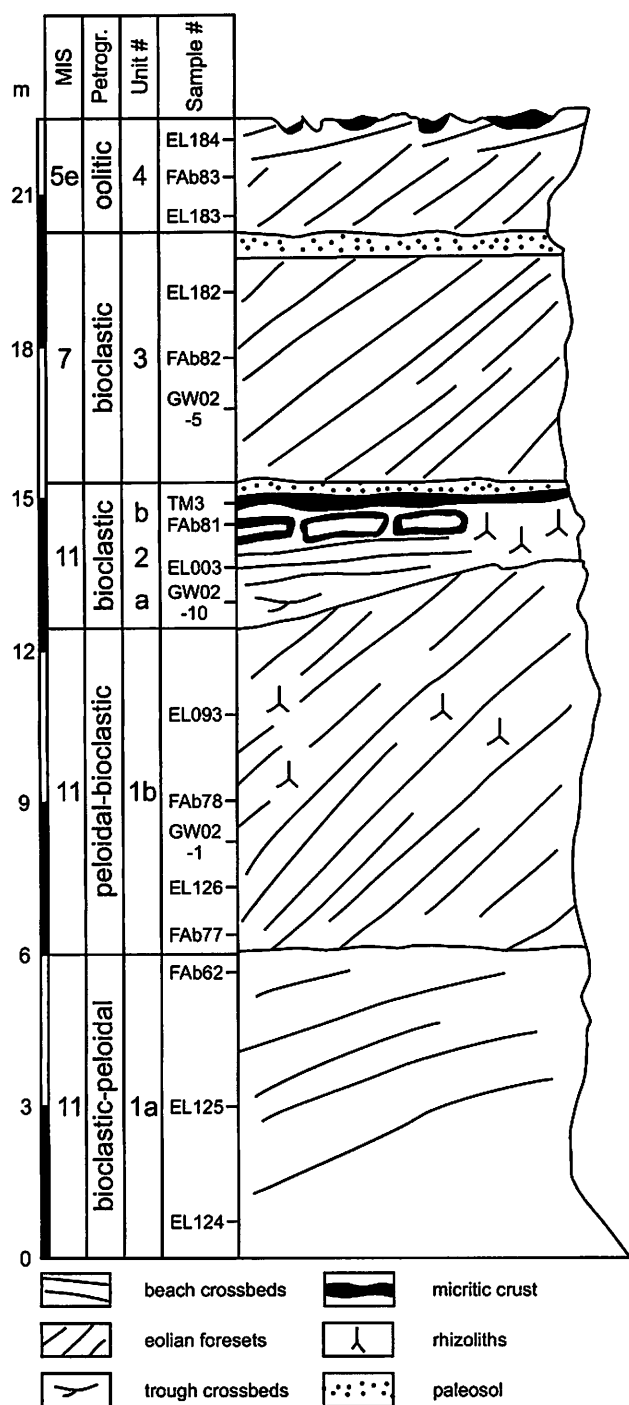
Figure 5: Stratigraphic log of the GW1 section. Column headings: Petrogr. = petrography; MIS = Marine isotope stage. EL, FAb, GW, and TM samples were collected by P. Kindler, F. Godefroid, C. Nawratil de Bono and T. Michaud, respectively.

undulating laminae (Fig. 11a): (1) light-coloured, porous laminae, commonly including carbonate allochems and filamentous structures with a cellular texture (Fig. 11b), and (2) dark, dense, micritic laminae, comprising peculiar, micron-scale, spherical to elongated calcitic bodies interpreted as spherulites of cyanobacterial origin (Fig. 11c; Verrecchia et al., 1995). These features can be isolated or occur in bundles, and consist of radially arranged calcite needles, showing a black cross in cross-polarized light.

Overlying and capped by a dm-thick, sandy paleosol, Unit 3 is about 5 m thick (Figs. 3 and 5). It is made of a moderately lithified, bioclastic limestone, showing large foresets dipping towards the bank interior with a ca. 30° angle. This rock is essentially composed of bioclasts, often leached or micritized, among which benthic foraminifers (miliolids, rotaliids) and red-algal fragments are predominant. No ooids and very few peloids have been observed in thin section. Constituent grains are bound by gravitational and meniscus cements composed of equant crystals of low-Mg calcite.

Unit 4 forms the upper 2 m of the GW 1 section and becomes somewhat thinner bankwards. It overlies a sandy paleosol and its upper boundary corresponds to a karstic surface (Figs. 3 and 5). It consists of a medium-grained, well-lithified, oolitic-peloidal grainstone, showing large foresets dipping towards the SW near its base, and subhorizontal beds near its top. Ooids, most of which are partly calcified, and peloids represent up to 60% of the constituent grains. Intergranular pores are filled by an equant to drusy mosaic of low-Mg calcite crystals. Scattered rhizoliths can further be observed in this unit.

Section GW2 (Figs. 4 and 12) is an ~4 m-high road cut showing three vertically stacked carbonate units. Road level is at about 13 m above sea level. The ocean-facing cliff below the road is not accessible without climbing gear. On the lagoon-facing slope, rocks are altered and karstified, and not suitable for sedimentological and petrographic examination.
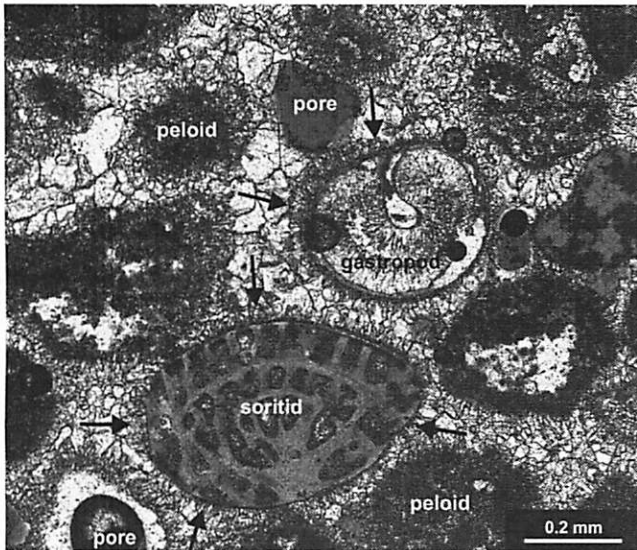
Figure 6: Sample EL 125, GW 1 section, see Fig. 5 for sample location. Thin-section view of biopeloidal grainstone forming Unit 1a. Note partly preserved early generation of fibrous or bladed rim cement (black arrows) enclosed in late drusy mosaic (Flügel, 2004). Although calcitized, the rim cement shows that early diagenesis took place in a phreatic, probably marine setting. Note also that calcite crystals of the drusy mosaic increase in size towards pore centers and commonly exhibit plane intercrystalline boundaries. These features, as well as the good preservation of constituent grains (e.g. soritid fragment), indicate this calcite is a primary phreatic cement and not of neomorphic origin (Bathurst, 1975).
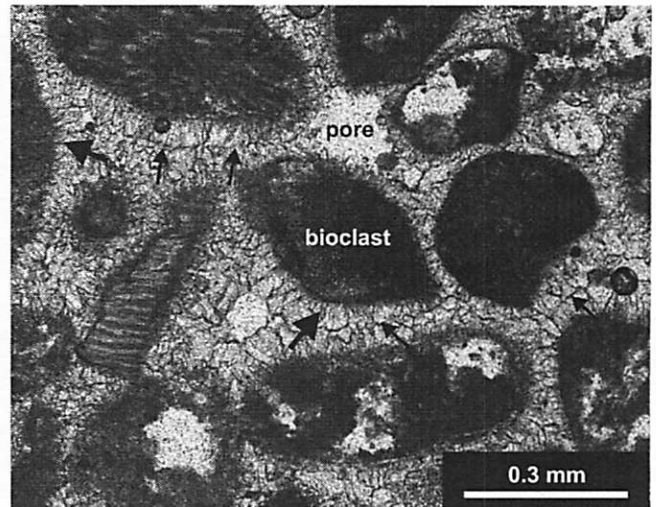
Figure 7: Sample GW02-1, GW1 section, see Fig. 5 for sample location.. Thin-section view of biopeloidal grainstone forming Unit 1b. Note important micritization of grains, early generation of fibrous/bladed rim cement (thick arrows) enclosed in late sparry calcite crystals forming polygonal compromise boundaries (thin black arrows). The latter form when crystals growing from adjacent grains meet, and characterize a phreatic diagenetic environment (Harwood, 1988).

Unit A forms the lower 1 to 1.2 m of the road cut. Its base is hidden below road level, and its top corresponds to a sharp erosional surface (Figs. 4 and 12). It consists of a well-lithified, pedogenized, peloidal-bioclastic grainstone showing planar and curved bedding (Fig. 4), and containing abundant traces of fossil vegetation (roots, trunks). Fossil nebkhas (coppice dunes) (Plaziat and Mahmoudi, 1990) and fenestral porosity can be locally observed in this unit. Predominant bioclasts include *Halimeda* fragments and benthic foraminifers. Grains are bound by an early generation of fibrous rim cement, partly altered by

a younger equant to drusy calcite mosaic, which fills most of the remaining pore spaces.

About 1.2 m thick, Unit B overlies the aforementioned erosional surface. It is capped by a red sandy-clayey paleosol, and can be subdivided into two units (B1 and B2). Unit B1 is made of well-lithified, coarse-grained, laminated, bioclastic grainstone, displaying planar crossbeds dipping towards the bank interior with a low angle. The upper part of this unit is dismantled into dm-sized polygonal blocks (Fig. 13). These rocks are rich in *Halimeda* fragments and large benthic foraminifers, such as Peneroplidae, Soritidae and Miliolidae, and further contain peloidal grainstone clasts, likely derived from the underlying unit. Grains are cemented by a first generation of calcitized fibrous rims, covered by a thin micritic film locally forming bridges between adjacent

particles, and a late generation of drusy calcite mosaic partly filling the remaining porosity (Fig. 14). Unit B2 is a cm-thick laminated crust, that caps and penetrates the upper 50 cm of Unit B1. In thin section, this crust shows an alternation of mm-scale, dense micritic and porous laminae, the former containing numerous calcite spherulites. This crust is identical to that forming Unit 2b at GW1 (Fig. 11).

Unit C is about 1 to 1.5 m thick (Figs. 4 and 12). It overlies the aforementioned paleosol and is capped by a deeply karstified surface. It consists of a fine-grained oolitic-peloidal grain-stone exhibiting steep foresets dipping towards the bank interior and numerous rhizoliths. Most ooids have been partly calcified and/or leached. Cement amounts to about 40% of the rock volume and is represented by a drusy calcite mosaic.

Geochronology

Table 1 presents the values of A/I ratios obtained by Hearty (1998) and Nawratil de Bono (2008) from the Glass Window area. Both authors studied and sampled the GW1 section, whereas the GW2 section was only examined by Nawratil de Bono (2008).

INTERPRETATIONS

Paleo-depositional and diagenetic environments

The carbonate units exposed at section GW1 can be interpreted as follows:

Unit 1: The occurrence of m-scale foresets dipping towards the bank interior (Figs. 3 and 5), the overall good sorting of grains, and the presence of an intervening pedogenic zone between Units 1a and 1b, all indicate that Unit 1 was formed in
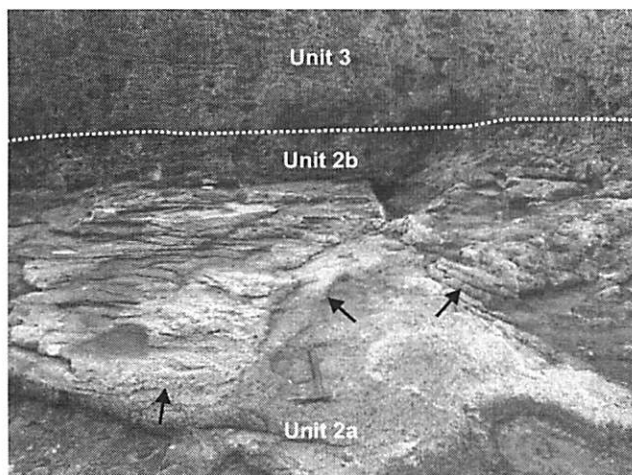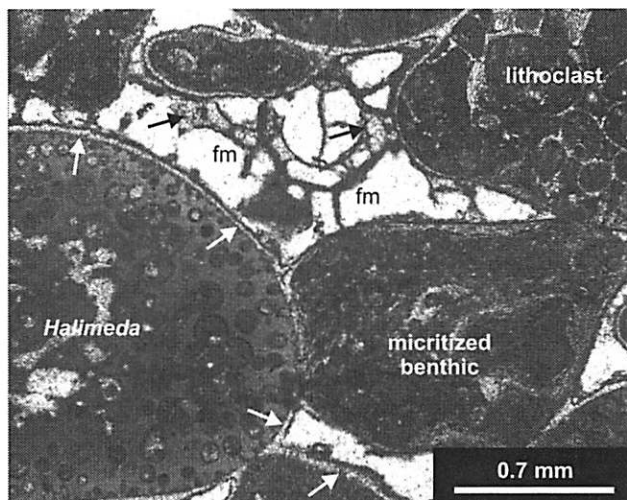

Figure 8: Trough cross-strata (arrows) exposed near the base of Unit 2a at GW1. Irregular lower bounding surface (right and beneath the hammer) suggests these crossbeds were produced by wave action (compare with Reineck and Singh, 1980, p. 34). Dotted line emphasizes the boundary between Unit 2b and 3; hammer length = 36 cm.

Figure 9: Sample EL 003, GW1 section, see Fig. 5 for sample location.. Thin-section view of Unit 2a microfacies. Note lithoclast of peloidal grain-stone, probably reworked from Unit 1, enclosed in coarse bioclastic grainstone rich in Halimeda grains. Note also early rim cement (white arrows), filamentous micrite (fm) in empty pore spaces, and rare sparry mosaic filling interstices between mi-critic bridges (black arrows).
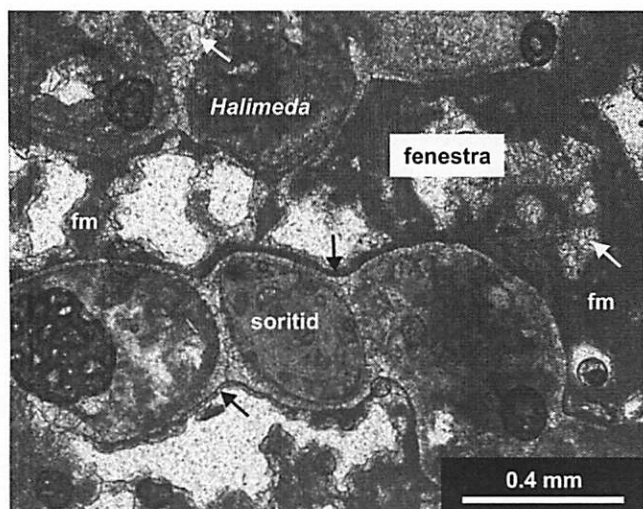
Figure 10: Sample GW02-10, GW1 section, see Fig. 5 for sample location. Closer view of the three superimposed cements occurring in Unit 2a: 1) moderately preserved early isopachous rims (black arrows), 2) filamentous micrite (fm), 3) late blocky spar (white arrows). Note the central pore is much larger than surrounding grains and can thus be identified as a fenestra. Preserved rim cement includes ghosts of fibrous crystals suggesting early diagenesis took place in a marine phreatic environment (Harris et al, 1985). The filamentous micrite could be related to microbial processes.
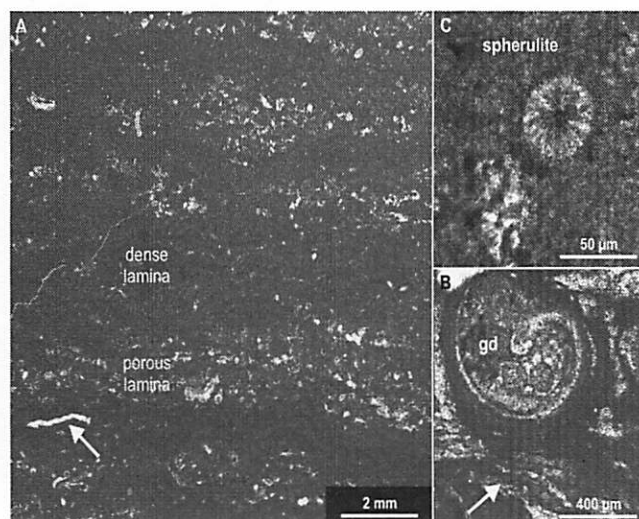

Figure 11: Sample TM3, GW1 section, see Fig. 5 for sample location. Oriented (top is up) thin-section view of one laminated crust forming Unit 2b. A. Microscopic view illustrating the two types of mm-scale, undulating laminae forming this unit; white arrow points to one elongated pore interpreted as a horizontal dessication crack. B. Closer view of porous lamina showing one gastropod fragment (gd) and a filamentous structure with a cellular texture (white arrow) interpreted as an algal remain. C. Close-up on dense, micritic lamina showing fibro-radial spherulites of cynobacterial origin.

a supratidal setting. Constituent particles were probably derived from a low-energy lagoonal environment, where porcellaneous foraminifers and green algae thrived, and were then deposited on a coastal dune. Interestingly, the diagenetic history of this eolianite took place, first, in a marine phreatic zone, as illustrated by the preserved early fibrous rim cement (Fig. 6), and then in a freshwater phreatic setting, as shown by the late drusy calcite mosaic and polygonal compromise boundaries (Fig. 7).

Unit 2a: The presence of trough-cross bedding (Fig. 8), low-angle planar cross-stratification, rare fenestral porosity, as well as the coarse grain size suggest an upper subtidal to intertidal paleodepositional setting for this unit, which is further

corroborated by the early generation of fibrous rim cement, typical of the marine phreatic diagenetic realm (Figs. 9 and 10; Harris et al., 1985).

Unit 2b: The beige to brown crust forming this unit could tentatively be interpreted as a pedogenic calcrete, which would be coherent with the presence of the overlying paleosol. However, the alternation of porous laminae, commonly including carbonate allochems and filamentous structures with a cellular texture (Fig. 11b), and of dense laminae comprising spherulites of cyanobacterial origin (Fig. 11c), as well as the scarcity of typical pedogenic structures, rather suggest this layer corresponds to a fossil, low-energy, lacustrine (or pond) deposit formed under the influence of algal and cyanobacterial activity. These require

light, and therefore rule out that this crust formed at a certain depth in the sediment, as pedogenic calcrete does. This horizon presents many resemblances with the modern lacustrine deposits observed at Storr's Lake on San Salvador (Neumann et al., 1988). There, cyanobacterial/algal mats are closely associated with fine-grained, detrital carbonate sediment, forming undulating, mm-thick laminae very similar to those found in Unit 2b (Fig. 15). The latter also resemble the modern cyanobacterial mats observed on older beach deposits at James Pond (Eleuthera; Nawratil de Bono, 2008).

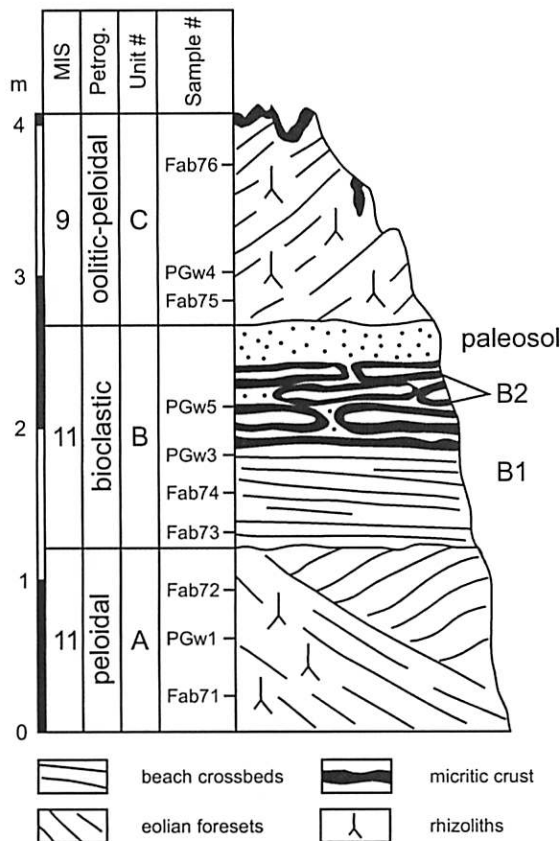Units 3 and 4: Large landward-dipping cross stratifications, occasional root traces, and
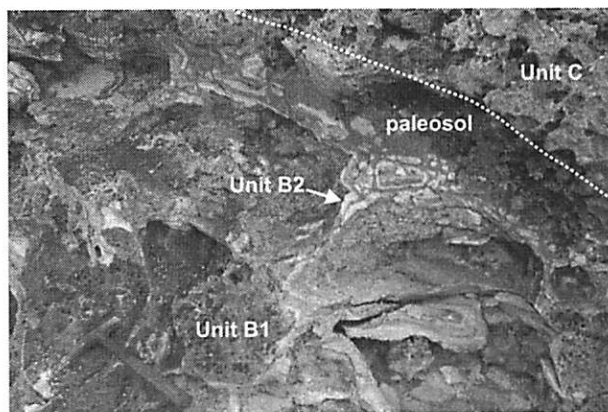

Fig. 13: Oblique view of the boundary between Units B and C at the GW2 section. Note from bottom to top (i.e. left to right): (1) fragmented upper part of Unit B1; (2) Unit B2 crust covering the dismantled blocks; (3) overlying sandy paleosol; and (4) base of Unit C. Hammer for scale is 36 cm long.

Figure 12: Stratigraphic log of the GW2 section. Column headings: Petrogr. = petrography; MIS = Marine isotope stage. FAb and PGw samples were collected by F. Godefroid and C. Nawratil de Bono, respectively.

widespread low-Mg calcite cements identify the uppermost two units at GW1 as eolianites. The constituent grains of Unit 3, dominated by benthic foraminifers, red-algal and coral fragments, were probably derived from a reefal environment, whereas those forming Unit 4 (ooids and peloids) originated most probably from an ooid shoal.

At section GW2, Unit A can be interpreted as an eolianite, based on the occurrence of large-scale cross-bedding, good sorting of constituent grains, and the presence of numerous traces of fossil vegetation (nebkhas). Note that diagenesis of this unit first occurred in a marine phreatic setting (early fibrous rim cement), and then in the meteoric phreatic zone (late drusy low-Mg calcite). Unit B1 likely corresponds to a fossil beach, as indicated by low-angle planar cross-beds (Figs. 4 and 12), fenestral porosity, coarse grain size, and early fibrous rim-cements (Fig. 14). The upper part of this unit is dismantled into dm-sized polygonal blocks (Fig. 13), as is the case for many modern beachrocks. Unit B2 was probably deposited in a low-energy lacustrine environment characterized by undulating algal and cyanobacterial mats. Fi-

nally, Unit C is identified as an eolianite because of the presence of steep, landward dipping fore-sets, rhizoliths, and early low-Mg calcite cement. The constitutive particles of this unit (ooids and peloids) originate from an ooid shoal.

Age and correlation of stratigraphic units

Knowing that, in the Bahamas, terra-rossa paleosols usually separate carbonate deposits formed during distinct interglacial sea-level high-stands (Carew and Mylroie, 1997), and applying the basic principle of stratigraphic superposition, the following correlations can be proposed. At GW1, Units 1 and 2 occur below one paleosol supporting two paleosol-capped carbonate units (Units 3 and 4; Figs. 3 and 5). Providing none of these paleosols is composite, or bifurcates (Carew and Mylroie, 1991), Units 1 and 2 could thus be
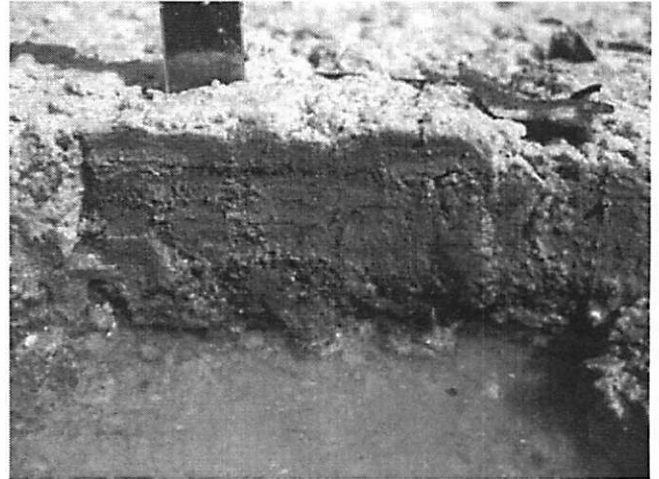

Figure 15: Box core made through modern algal/ cyanobacterial mats in Storr's Lake, San Salvador. Width of spatula is 3 cm.

Figure 14: Sample FAb 74, GW2 section, see Fig. 12 for sample location. Thin-section view of Unit B1 microfacies. Note large Halimeda fragments. Cement succession includes: (1) recrystallized, isopachous fibrous cement rimming the grains (white arrows), (2) undulating micrite forming locally bridges between particles (black arrows), and (3) drusy calcite mosaic (dcm) partly filling the remaining pore spaces. Compare with Figs. 9 and 10.

attributed to MIS 9. Following the same reasoning, Units 3 and 4 could be correlated with MIS 7 and MIS 5e, respectively. By the same token, Units A and B, at GW2, could be correlated with MIS 7 and Unit C with MIS 5e. Consideration of the amino-acid racemization data presented by Hearty (1998) and Nawratil de Bono (2008) leads to a somewhat different interpretation.

Except for one specimen collected at the base of the section (Table 1), samples gathered from Units 1 and 2, at GW1, yielded A/I ratios between 0.616 and 0.707, suggesting a correlation with Aminozones G/H (Hearty and Kaufman, 2000), which span MIS 9 and 11. The reversed stratigraphic order of the ratios obtained from Unit 1 (0.674, 0.616) and Unit 2 (0.707) could be linked to a temperature effect due to the superficial location of the sample collected from Unit 2. A/I values obtained from Unit 3 range between 0.467 and 0.581, indicating a correlation with Aminozone F, or MIS 7 (Hearty and Kaufman, 2000), which is consistent with the stratigraphy. Hearty (1998) reports an A/I value of 0.569 for Unit 4, suggesting also a correlation with MIS 7. However, the analyzed sample is a bioclastic grainstone (Table 1; Hearty, 1998), which could have been picked
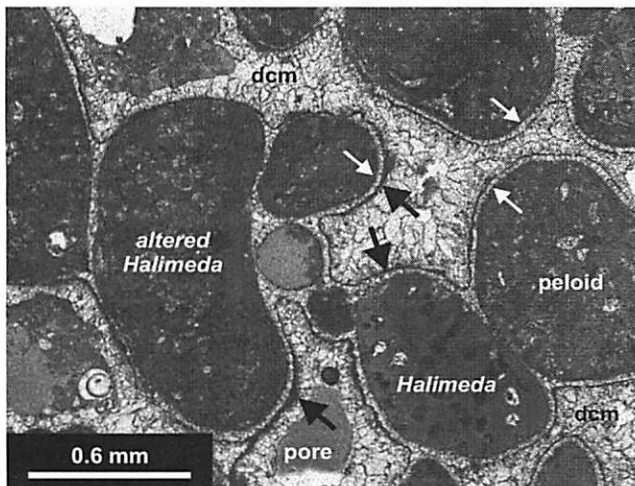
up from Unit 3, rather than from Unit 4, which is oolitic. The A/I ratios of all stratigraphic units exposed at GW2 range between 0.757 and 0.652, and could thus be correlated with Aminozones G/H (Hearty and Kaufman, 2000), i.e. with MIS 9-11. We correlate Units A and B with MIS 11 and Unit C with MIS 9, because the latter overlies a terra-rossa paleosol capping Unit B (Figs. 4, 12 and 13).

Based on their stratigraphic position, petrographic and sedimentological characteristics, and amino-acid content, we correlate the units exposed at GW1 and GW 2 as follows (Fig. 16). The bio-peloidal eolianites forming the base of both sections (Unit 1 and Unit A) can be correlated, and attributed to MIS 11. Units 2 and B, both of which consist of beach and lacustrine sediments, were deposited at a later time during this same interglacial. Unit C (oolitic-peloidal eolianite), which pinches out between GW2 and GW1, is attributed to MIS 9. Units 3 (bioclastic eolianite) and 4 (oolitic-peloidal eolianite) have no equivalents at GW2, and represent MIS 7 and MIS 5e, respectively.
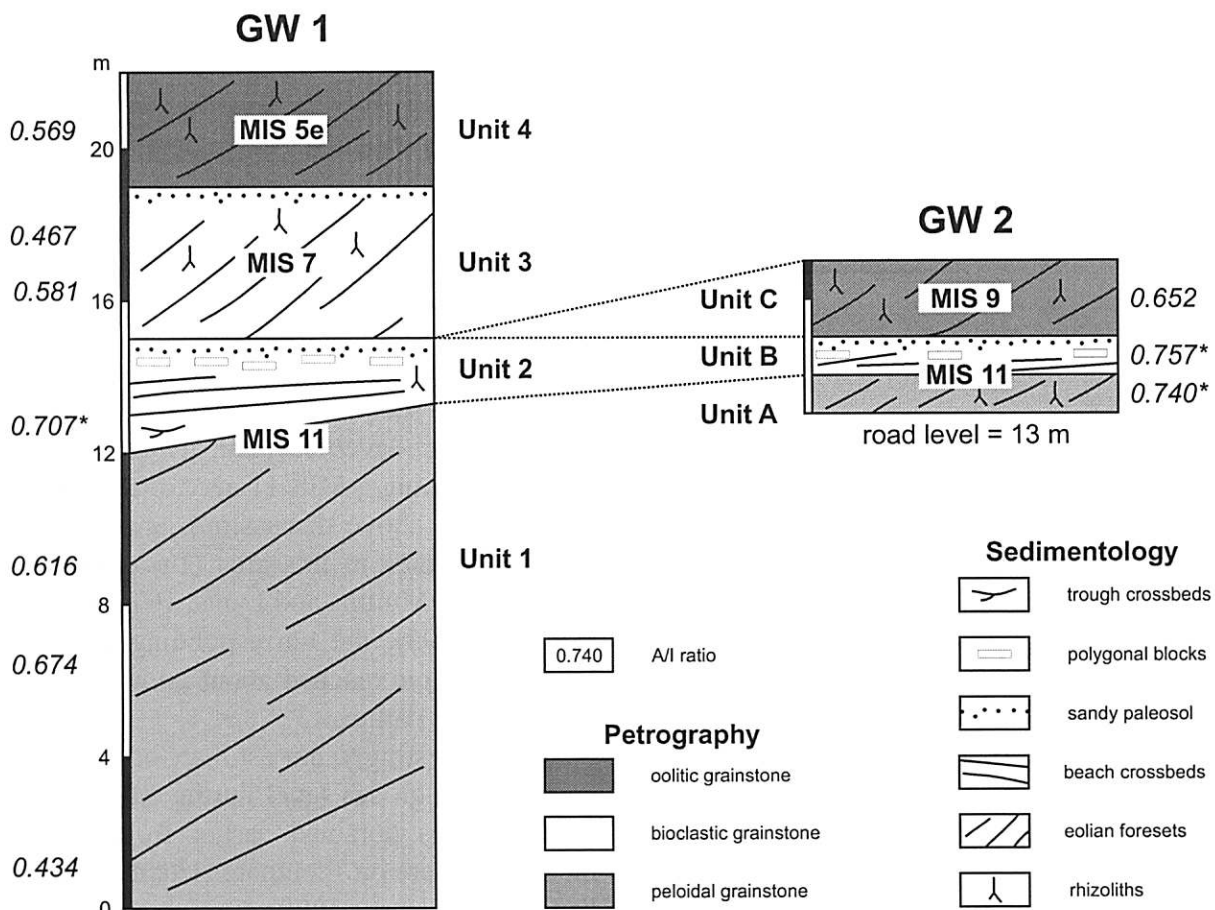

Figure 16: Stratigraphic correlations between sections GW1 and GW2. Asterix to the right of A/I ratio indicates that value might be slightly elevated due to a temperature effect. Anomalously low ratio of sample collected near the cliff base at GW1 could be related to contamination by recent organic material.

Table 1: Amino-acid racemization data (alloisoleucine/isoleucine ratios) compiled from Hearty (1998; PJH) and Nawratil de Bono (2008; CDB). Oo. = oolitic; pel. = peloidal, bio. = bioclastic; c. = coarse-grained.

Glass Window 1					
	Author	Sample	Av. value	Δ	Petrography
Unit 4	PJH	EGW1h	0.569	0.022	bioclastic
Unit 3					
	CDB	GW02-5	0.467	0.028	bioclastic
	PJH	EGW1f	0.581	0.023	bioclastic
Unit 2	CDB	GW02-10	0.707	0.016	c. bio.
Unit 1b					
	PJH	EGW1d	0.616	0.021	pel.-bio.
	CDB	GW02-1	0.674	0.010	pel.-bio.
Unit 1a	PJH	EGW1c	0.434	0.013	bio.-pel.
Glass Window 2					
Unit C	CDB	PGW02-4	0.652	0.032	oo.-pel.
Unit B	CDB	PGW02-3	0.757	0.037	c. bio.
Unit A	CDB	PGW02-1	0.740	0.042	pel.-bio.

Implications for sea-level history

The most salient observation made in the Glass Window area is the occurrence, at both studied sections, of sedimentological and early diagenetic features indicative of both a high sea level and an elevated water table, likely associated with the former. These features include (1) isopachous fibrous cements, drusy calcite mosaic and polygonal compromise boundaries found throughout Units 1 and A (Figs. 6 and 7); (2) trough cross-stratification, beach bedding, fenestral porosity and early fibrous rim cement occurring in Units 2a and B1 (Figs. 8, 9, 10 and 14), and (3) fossil algal and cyanobacterial mats forming Units 2b and B2 (Figs. 11 and 13). We suggest that all these features were formed during one episode of high sea level coeval with the deposition of the subtidal to intertidal deposits (Units 2a and B1) and overlying lacustrine/pond sediments (Units 2b and B2) constituting Units 2 and B. The top of this shal-lowing-upward sequence of facies is found at 15 masl at both sections. This value corresponds to the relative sea-level elevation at the time of deposition. Assuming a MIS 11 age for these deposits (refer to the above discussion), and considering subsidence rates in this area (1.6 cm/10^3 years; Lynts, 1970; Mullins and Lynts, 1977; Carew and Mylroie, 1995), the corresponding eustatic sea level must have reached about 20 m above modern ordnance datum.

Interestingly, our estimate of +20 m for an episode of high sea level during MIS 11 matches the values obtained earlier from beach terraces elsewhere on Eleuthera (Hearty et al. 1999; Kindler and Hearty, 2000), from an elevated, cave-filling, marine conglomerate in Bermuda (Land et al., 1967; Hearty et al. 1999; Kindler and Hearty, 2000; Hearty and Olson, 2008; Olson and Hearty, 2009), from perched phreatic caves on Middle Caicos (Caicos Platform; Smart et al. 2008), and, after deduction of regional uplift, from elevated

coral heads in Oahu (Hawaii; Hearty, 2002, 2007). The appealing aspect of the Glass Window data, particularly of the perched low-energy lacustrine/ pond deposits and of the elevated phreatic cements, is that they cannot be interpreted as high-energy tsunami or storm deposits, as has been the case for the Bermuda conglomerate (McMurtry et al., 2008) and the Eleuthera beaches (Mylroie, 2008). In addition, the subsiding tectonic regime affecting the NE portion of Great Bahama Bank indicates that, unlike the Hawaiian corals, the studied stratigraphic units have not been uplifted.

CONCLUSIONS

The present paper provides a detailed sedimentological and petrographic analysis of the complex stack of carbonate units exposed in the Glass Window area, one of the most spectacular rock outcrops in the Bahamas. Of prime interest is the discovery of fossil algal and cyanobacterial crusts, typical of lacustrine and pond environments, that have never been described, up to now, in the stratigraphic record of the Bahamas islands. These crusts must not be confused with pedogenic calcretes, to which they resemble, because their stratigraphic significance is entirely different: the latter reflect periods of interrupted carbonate sedimentation on the banks, possibly linked to sea-level lowstands, whereas the former correspond to times of elevated sea levels.

The perched beach and lacustrine/pond sediments exposed at GW1 and GW2, as well as the pervasive phreatic cements observed in the underlying eolianites, indicate that sea level rose to an elevation of about 20 masl during the middle Pleistocene. Based on basic stratigraphic principles and amino-acid racemization data, the occurrence of this exceptional sea-level highstand can be best correlated with MIS 11, about 400 ka BP, and thus further supports similar observations made at several locations worldwide.

Finally, and in the perspective of modern global warming, one has to remember that the Earth's orbital parameters were about the same during MIS 11 as during the present interglacial (MIS 1; Ruddiman, 2005). Climatic conditions and climate evolution during these two periods can thus be compared. The collapse and partial melting of polar ice sheets, and the subsequent sea-level increase at 20 masl occurred at the end of MIS 11, and was probably linked to its exceptional duration (20 to 35,000 yrs). MIS 1 began only 12,000 years ago, and thus, the prospect of a 20 m rise in sea level appears rather remote in time. However, the present-day, human-induced increase in atmospheric greenhouse gases may drastically accelerate the disintegration of polar ice-sheets, causing a catastrophic elevation of sea level in the next centuries. The MIS 11 stratigraphic record from the Bahamas shows that this is possible.

ACKNOWLEDGMENTS

REFERENCES

Bain, R.J., and Foos, A.M., 1993, Carbonate microfabrics related to subaerial exposure and paleosol formation, in Rezak, R., and Lavoie, D.L., eds, Carbonate Microfabrics: Springer, New York, p. 19-27.

Ball, M.M., 1967, Carbonate sand bodies of Florida and the Bahamas: Journal of Sedimentary Petrology, v. 37, p. 556-591.

Bathurst, R.G.C., 1975, Carbonate sediments and their diagenesis: Developments in Sedimentology, v. 12, Elsevier, Amsterdam, 658 pp.

Bowen, D.Q., 1999, +23 m stage 11 sea-level in Southern Britain, in Poore, R.Z., Burckle, L., Droxler, A., and McNulty, W.E., eds, Marine Oxygen Isotope Stage 11 and associated terrestrial records: workshop report: U.S. Geological Survey Open-File Report, 99-312, p.15-17.

Brigham-Grette, J., 1999: Marine Isotope Stage 11 high sea level record from Northwest Alaska, in Poore, R.Z., Burckle, L., Droxler, A., and McNulty, W.E., eds, Marine Oxygen Isotope Stage 11 and associated terrestrial records: workshop report: U.S. Geological Survey Open-File Report, 99-312, p.19-21.

Carew, J.L., and Mylroie, J.E., 1991, Some pitfalls in paleosol interpretation in carbonate sequences: Carbonates and Evaporites, v. 6, p. 69-74.

Carew, J.L. and Mylroie, J.E., 1995, Quaternary tectonic stability of the Bahamian archipelago: evidence from fossil coral reefs and flank margin caves: Quaternary Science Reviews, v. 14, p. 145-153.

Carew, J.L., and Mylroie, J.E., 1997, Geology of The Bahamas, in Vacher, H.L., and Quinn, T.M., eds, Geology and hydrogeology of carbonate islands: Developments in Sedimentology, v. 54, Elsevier, Amsterdam, p. 91-139.

Droxler, A.W., Poore, R.Z., and Burckle, L., 1999, Data on past climate warmth may lead to better model of warm future. EOS, Transaction, American Geophysical Union, v. 80 (26), p. 289-290.

Flügel, E., 2004, Microfacies of carbonate rocks: Springer Verlag, Berlin, 976 pp.

Hagey, F.M., and Mylroie, J.E., 1995, Pleistocene lake and lagoon deposits, San Salvador Island, Bahamas, in Curran, H.A. and White, B., Terrestrial and Shallow Marine Geology of the Bahamas and Bermuda: Geological Society of America Special Paper 300, p. 77-90.

Harris, P.M., Kendall, C.G.St.C., Lerche, I., 1985, Carbonate cementation - a brief review, in Schneidermann, N., and Harris, P.M., eds, Carbonate cements: SEPM Special Publication 36, p. 79-95.

Harwood, G., 1988, Microscopical techniques: II. Principles of sedimentary petrography, in Tucker, M., ed., Techniques in Sedimentology: Blackwell Scientific Publications, p. 86 -107.

Hearty, P.J., 1997, Boulder deposits from large waves during the last interglaciation on North Eleuthera Island, Bahamas: Quaternary Research, v. 48, p. 326-338.

Hearty, P.J., 1998, The geology of Eleuthera island, Bahamas: a rosetta stone of Quaternary stratigraphy and sea-level history: Quaternary Sciences Reviews, v. 17, p. 333-355.

Hearty, P.J., 2002, The Ka'ena highstand of O'ahu, Hawai'i: further evidence of Antarctic ice collapse during the middle Pleistocene: Pacific Science, v. 56, p. 65-81.

Hearty, P.J., 2007, MIS 11 rocks! The "smoking gun" of a catastrophic +20 m eustatic sea-level rise: PAGES News, v.15, p. 25-26.

Hearty, P.J., and Kaufman, D.S., 2000, Whole-rock aminostratigraphy and Quaternary sea-level history of the Bahamas: Quaternary Research, v. 54, p. 163-173.

Hearty, P.J., Kindler, P., Cheng, H. and Edwards, R.L., 1999, A +20m middle Pleistocene sea-level highstand (Bermuda and the Bahamas) due to partial collapse of Antarctic ice: Geology, v. 27, p.375-378.

Hearty, P.J., and Olson, S.L., 2008, Mega-high-stand or megatsunami? Discussion of McMurtry et al. (Elevated marine deposits in Bermuda record a late Quaternary megatsunami: Sed. Geol. 200 (2007) 155-165): Sedimentary Geology, v. 203, p. 307-312.

Hearty, P.J., Vacher, H.L., and Mitterer, R.M., 1992, Aminostratigraphy and ages of Pleistocene limestones of Bermuda: Geological Society of America Bulletin, v. 104, p. 471-480.

Hodell, D.A., Charles, C.D., and Ninnemann, U.S., 2000, Comparison of interglacial stages in the South Atlantic sector of the southern ocean for the past 450 kyr: implications for Marine Isotope Stage (MIS) 11: Global and Planetary Change, v. 24, p. 7-26.

Howard, W.R., 1997, A warm future in the past: Nature, v. 388, p. 418-419.

Kandiano, E.S., and Bauch, H.A., 2007, Phase relationship and surface water mass change in the Northeast Atlantic during Marine Isotope Stage 11 (MIS 11). Quaternary Research, v. 68, p. 445-455.

Kindler, P. and Hearty, P.J., 1995, Pre-Sangamonian eolianites in the Bahamas? New evidence from Eleuthera Island: Marine Geology, v. 127, p. 73-86.

Kindler, P., and Hearty, P.J., 1996, Carbonate petrography as an indicator of climate and sea-level changes: new data from Bahamian Quaternary units: Sedimentology, v. 43, p. 381-399.

Kindler, P., and Hearty, P.J., 1997, Geology of The Bahamas: architecture of Bahamian Islands, in Vacher, H.L., and Quinn, T.M., eds, Geology and hydrogeology of carbonate islands: Developments in Sedimentology, v. 54, Elsevier, Amsterdam, p. 141-160.

Kindler, P., and Hearty, P.J., 2000, Elevated marine terraces from Eleuthera (Bahamas) and Bermuda: sedimentological, petrographic and geochronological evidence for important deglaciation events during the middle Pleistocene: Global and Planetary Change, v. 24, p. 41-58.

Land, L.S., MacKenzie, F.T., and Gould, S.J., 1967, Pleistocene history of Bermuda: Geological Society of America Bulletin, v. 78, p. 993-1006.

Lynts, G.W., 1970, Conceptual model of the Bahamian platform for the last 135 million years: Nature, v. 225, p. 1226-1228.

Masaferro, J.L., Poblet, J., Bulnes, M., Eberli, G.P., Dixon, T.H., and McClay, K., 1999, Palaeogene-Neogene/present day(?) growth folding in the Bahamian foreland of the Cuban fold and thrust belt: Journal of the Geological Society, London, v. 156, p. 617-631.

McMurtry, G.M., Tappin, D.R., Sedwick, P.N., Wilkinson, I., Fietzke, J., and Sellwood, B., 2008, Elevated marine deposits in Bermuda record a late Quaternary megatsunami: Sedimentary Geology, v. 200, p. 155-165.

Michaud, T., 1999, Géologie, stratigraphie et étude physico-chimique des paléosols de la région de North-Eleuthera (Bahamas): Unpublished M.S. thesis, University of Geneva, 91 pp.

Mullins, H.T., and Lynts, G.W., 1977, Origin of the northeastern Bahama Platform: Review and reinterpretation: Geological Society of America Bulletin, v. 88, p. 1447-1461.

Mylroie, J.E., 2008, Late Quaternary sea-level position: evidence from Bahamian carbonate deposition and dissolution cycles: Quaternary International, v. 183, p. 61-75.

Nawratil de Bono, C., 2008, Pétrographie, micromorphologie et minéralogie des paleosols pléistocènes d'Eleuthera, Bahamas: enseignements paléoclimatiques, stratigraphiques et sédimentologiques : Terre & Environnement, v. 75, 26 pp. + CD-Rom.

Neumann, C.A., Bebout, B.M., McNeese, L.R., Paull, C.K., and Paerl, H.A., 1988, Modern stromatolites and associated mats: San Salvador, Bahamas, in Mylroie, J.E., ed., Proceedings of the 4th Symposium on the Geology of the Bahamas: Bahamian Field Station, San Salvador, p. 235-251.

Noble, R.S., Curran, H.A., and Wilson, M.A., 1995, Paleoenvironmental and paleoecologic analyses of a Pleistocene mollusc-rich lagoonal facies, San Salvador Island, Bahamas, in Curran, H.A. and White, B., Terrestrial and Shallow Marine Geology of the Bahamas and Bermuda: Geological Society of America Special Paper 300, p. 91-103.

Olson, S.L., and Hearty, P.J., 2009, A sustained +21 m sea-level highstand during MIS 11 (400 ka): direct fossil and sedimentary evidence from Bermuda: Quaternary Science Reviews, v. 28, p. 271-285.

Panuska, B.C., Boardman, M.R., Carew, J.L., Mylroie, J.E., Sealey, N.E., Voegeli, V., 2002, Eleuthera Island field trip Guide, 11th Symposium on the Geology of the Bahamas

and Other Carbonate Regions: Gerace Research Center, San Salvador Island, Bahamas, 20 pp.

Pindell, J.L., 1985, Alleghenian reconstruction and subsequent evolution of the Gulf of Mexico, Bahamas, and proto-Caribbean: Tectonics, v. 4, p. 1-39.

Plaziat, J.C., and Mahmoudi, M., 1990, The role of vegetation in Pleistocene eolianite sedimentation: an example from Eastern Tunisia: Journal of African Earth Sciences, v. 10, p. 445-451.

Poore, R.Z., Burckle, L., Droxler, A., and McNulty, W.E., 1999, Marine Oxygen Isotope Stage 11 and associated terrestrial records: workshop report: U.S. Geological Survey Open-File Report, 99-312, 79 pp.

Reineck, H.E., and Singh, I.B., 1980, Depositional sedimentary environments: Springer-Verlag, Berlin, 549 pp.

Ruddiman, W.F., 2005, Cold climate during the closest Stage 11 analog to recent millennia: Quaternary Science Reviews, v. 24, p. 1111-1121.

Sheridan, R.E., Mullins, H.T., Austin, J.A. Jr., Ball, M.M., and Ladd, J.W., 1988, Geology and geophysics of the Bahamas, in Sheridan, R.E., and Grow, J.A., eds., The Geology of North America, vol. I-2, The Atlantic Continental Margin: U.S. Geological Society of America, p. 329-364.

Smart, P.L., Moseley, G.E., Richards, D.A., and Whitaker, F.F., 2008, Past high sea-stands and platform stability: evidence from Conch Bar Cave, Middle Caicos, in Morgan, W.A., and Harris, P.M., eds, Developing models and analogs for isolated carbonate platforms

- Holocene and Pleistocene carbonates of Caicos Platform, British West Indies: SEPM Core Workshop 22, p. 203-210.

Verrecchia, E.P., Freytet, P., Verrecchia, K.E., and Dumont, J.L., 1995, Spherulites in calcrete laminar crusts: biogenic CaCO3 precipitation as a major contributor to crust formation: Journal of Sedimentary Research, v. A65, p. 690-700.